Environmental Science and Pollution Research (2018) 25:7647–7661
https://doi.org/10.1007/s11356-017-1105-9

RESEARCH ARTICLE

# Activated carbons from avocado seed: optimisation and application for removal of several emerging organic compounds

Anderson B. Leite[1] · Caroline Saucier[1] · Eder C. Lima[1] · Glaydson S. dos Reis[1,2] · Cibele S. Umpierres[1] · Beatris L. Mello[1] · Mohammad Shirmardi[3] · Silvio L.P Dias[1] · Carlos H. Sampaio[2]

Received: 21 August 2017 / Accepted: 19 December 2017 / Published online: 28 December 2017


## Abstract

In this study, avocado seed was successfully used as raw material for producing activated carbons by conventional pyrolysis. In order to determine the best condition to produce the activated carbons, a $2^2$ full-factorial design of experiment (DOE) with three central points was employed by varying the temperature and time of pyrolysis. The two evaluated factors (temperature and time of pyrolysis) strongly influenced the $S_{BET}$, pore volumes, hydrophobicity–hydrophilicity ratio (HI) and functional groups values; both factors had a negative effect over $S_{BET}$, pore volumes and functional groups which means that increasing the values of factors leads to decrease of these responses; on the other hand, with regards to HI, both factors caused a positive effect which means that increasing their values, the HI has an enhancement over its values. The produced activated carbon exhibited high specific surface areas in the range of 1122–1584 $m^2\ g^{-1}$. Surface characterisation revealed that avocado seed activated carbons (ASACs) have hydrophilic surfaces and have predominantly acidic groups on their surfaces. The prepared ASACs were employed in the adsorption of 25 emerging organic compounds such as 10 pharmaceuticals and 15 phenolic compounds which presented high uptake values for all emerging pollutants. It was observed that the activated carbon prepared at higher temperature of pyrolysis (700 °C), which generated less total functional groups and presented higher HI, was the activated carbon with higher sorption capacity for uptaking emerging organic contaminants. Based on results of this work, it is possible to conclude that avocado seed can be employed as a raw material to produce high surface area and very efficient activated carbons in relation to treatment of polluted waters with emerging organic pollutants.

**Keywords** Avocado seed · Design of experiments · Activated carbons · Emerging pollutants · Adsorption process

Responsible editor: Philippe Garrigues

**Electronic supplementary material** The online version of this article (https://doi.org/10.1007/s11356-017-1105-9) contains supplementary material, which is available to authorized users.

✉ Glaydson S. dos Reis
glaydson.simoes@ufrgs.br; glaydsonambiental@gmail.com

[1] Institute of Chemistry, Federal University of Rio Grande do Sul (UFRGS), Av. Bento Gonçalves 9500, P.O. Box 15003, Porto Alegre, RS 91501-970, Brazil

[2] School of Engineering, Department of Metallurgy, Federal University of Rio Grande do Sul (UFRGS), Av. Bento Gonçalves 9500, Porto Alegre, RS, Brazil

[3] Department of Environmental Health Engineering, Faculty of Paramedical Sciences, Babol University of Medical Sciences, Babol, Iran

## Introduction

Every year, large quantities of dangerous emerging organic pollutants are generated by many types of industries such petrochemical, medicines, textile, paper and plastics which consume a substantial number of phenolic compounds and pharmaceuticals which ends to produce a large amount of polluted water with their products (Ahmed et al. 2016; Geissena et al. 2015; Jiang et al. 2013).

These organic substances are delivered into wastewaters, and this brings serious issues for water contamination and its treatment, because it tends to persist even after the conventional removal processes in the wastewater treatment plants (Fatta-Kassinos and Michael 2013; Geissena et al. 2015). Therefore, their removal from industrial effluents has been a major environmental issue in recent years.

Several methods, such as advanced oxidation procedures (AOP) (Ba-Abbad et al. 2017; Gil et al., 2017, Lin et al. 2017a, b), biological treatment (Besha et al. 2017; Ghattas, et al., 2017), coagulation (Kishimoto and Kobayashi 2016), flocculation (Kishimoto and Kobayashi, 2016; Matamoros and Salvado 2013), filtration (Zhang et al. 2017b) and adsorption (Bhatnagar and Anastopoulos 2017; Zhuo et al. 2017) processes have been applied to remove this kind of pollutants from the effluents (Besha et al. 2017; Carmalin et al. 2016). Some of these methods have been shown to be effective; however, some of them presented some drawbacks and limitations such as an excess amount of chemical reagent, high implemental costs and high sludge production that has serious disposal problems. Among these methods, adsorption is a preferred route because of its low initial cost for implementation, simplicity and relatively low residue production (dos Reis et al. 2016a, b, 2017).

Adsorption technology using different adsorbents has been considered as one of the most efficient and economic method for treatment of effluents containing emerging organic pollutants such phenols and pharmaceuticals (Saucier et al. 2015, 2017; Thue et al. 2016, 2017). Accordingly, a large variety of adsorbent materials have been proposed and studied for their ability to remove emerging organic pollutants (Takdastan et al. 2016; Rossner et al. 2009; Prola et al. 2013b; Rovani et al. 2016). Among these adsorbents, activated carbon is one of the most employed adsorbents for adsorption of organic compounds simply because it has well-developed pore structures with high specific area that favours high adsorption ability (dos Reis et al. 2016c; Calvete et al. 2010; Ribas et al. 2014).

Nowadays, there is a great interest in finding effective adsorbents prepared from waste biomass (Leite et al. 2017; Prola et al. 2013a; Puchana-Rosero et al. 2017). Exploring efficiency and adding value to waste biomass may contribute to environmental sustainability and offer benefits for future commercial applications (Leite et al. 2017; Prola et al. 2013a; Puchana-Rosero et al. 2017).

For instance, Saucier et al. (2015) prepared an activated carbon (AC) from cocoa shell by using a mixture of zinc chloride plus iron chloride as agents of activation by using microwave-assisted pyrolysis. Then, the carbons were used for removal of sodium diclofenac and nimesulide from aqueous solutions; the maximum sorption capacities ($Q_{max}$) obtained were 63.47 and 74.81 $m^2\ g^{-1}$, for diclofenac and nimesulide, respectively, at 25 °C. In another study, Thue et al. (2016) reported the preparation of an AC from wood waste using microwave-assisted pyrolysis and the adsorbents were used for removal of o-cresol from aqueous solutions obtaining a $Q_{max}$ of 222.2 mg $g^{-1}$ at 25 °C. Ahmed et al. (2017) produced an AC from human hair using potassium hydroxide as activating agent, using a conventional furnace system for the pyrolysis. The prepared AC was used for the adsorption of tetracycline, and the $Q_{max}$ obtained was 128.52 $m^2\ g^{-1}$. Saucier et al. (2017) produced magnetic activated carbons by using iron and cobalt carboxylates, and the resulting adsorbents were used for removal of amoxicillin and paracetamol from aqueous solutions, obtaining $Q_{max}$ values of 339.4 and 302.2 $m^2\ g^{-1}$ for amoxicillin and paracetamol, respectively, at 25 °C.

Leite et al. (2017) prepared an AC from avocado seed using microwave-assisted pyrolysis, and the adsorbent was employed for removal of resorcinol and 3-aminophenol from aqueous solutions. The values of $Q_{max}$ obtained were 299.7 and 352.4 mg $g^{-1}$ for resorcinol and 3-aminophenol, respectively, at 25 °C. Although the microwave-assisted pyrolysis could present some advantages over the conventional furnace system (Puchana-Rosero et al. 2016), the microwave oven used for producing activated carbons is not commercially available, and it is usually an adaptation of domestic microwave oven that is used for pyrolysis of the biomass (Leite et al. 2017; Puchana-Rosero et al. 2016; Saucier et al. 2015, 2017; Thue et al. 2016, 2017). Therefore, these oven systems do not have available temperature control, and all the pyrolysis should be performed in the maximum power of the furnace. However, the conventional furnace for thermal pyrolysis is available, being possible to optimize several parameters, such as ramp heating rate, final temperature of pyrolysis, holding time at the final temperature and several steps of temperature for performing the pyrolysis.

However, for the preparation of activated carbons using pyrolysis of the biomass (Calvete et al. 2010; Ribas et al. 2014), there are some factors that might affect the final quality (porosity, surface chemistry and therefore the performance of adsorption) of the materials such as hold temperature and time (dos Reis et al. 2016c; Thue et al. 2017; Ribas et al. 2014). Then, a multivariate technique extensively and usefully is needed for applying in optimisation of procedures through fast, economic and effective pathway and allows more than one variable to be optimized simultaneously (Bruns et al. 2016; dos Reis et al. 2016c; Ennaciri et al. 2014). A good selection of design and optimisation models makes possible to simultaneously evaluate the variable contribution (main and interaction) on the preparation of a material with good adsorption properties (dos Reis et al. 2016c; Ennaciri et al. 2014).

In this work, the use of avocado seed has been studied for preparation of activated carbons (avocado seed activated carbon (ASACs)) and their preparations were optimized by using a $2^2$ full-factorial design of experiment (DOE) by varying two factors (temperature and time of pyrolysis) with three central points (total of seven experiments). The ASAC materials were characterized by $N_2$ adsorption–desorption isotherms, vibrational spectroscopy in the infrared region (FTIR), point of zero charge ($pH_{pzc}$), total acidic and basic groups, hydrophobicity–hydrophilicity ratio (HI). The quantitative parameters obtained were used as responses of the DOE, and then, the prepared ASACs were employed for adsorption of several emerging

organic compounds (10 pharmaceuticals and 15 phenolic compounds) from aqueous solutions.

## Material and method

### Statistics–experimental design

The design of experiment optimisation concerning the full-factorial design was carried out using Minitab version 17.3. Individual and synergetic effects of two operational parameters (see Table 1) including temperature of pyrolysis (A) and holding time (B) were investigated using a $2^2$ full-factorial design with three central points. The analysis of variance (ANOVA) was performed to justify the significance and adequacy of the developed regression model. The adequacy of the response surface models was evaluated by calculation of the adjusted determination coefficient ($R^2_{Adj}$), coefficient of variation, adequate precision and also by testing it for the lack of fit.

**Table 1** Optimisation of pyrolysis of avocado seed (AS) on conventional heating furnace. The $N_2$ flow was kept at 150 mL $min^{-1}$ during all the heating. When the heating program was cooled down, the $N_2$ was kept until the temperature was < 150 °C. Ramp temperature was used at 10 °C $min^{-1}$ from the room temperature until the final temperature ($T_f$)

| Experiment | Samples | $T_f$ (°C) | Hold time (min) |
|---|---|---|---|
| 1 | ASAC1 | 500 | 30 |
| 2 | ASAC2 | 700 | 30 |
| 3 | ASAC3 | 500 | 60 |
| 4 | ASAC4 | 700 | 60 |
| 5 | ASAC5 | 600 | 45 |
| 6 | ASAC6 | 600 | 45 |
| 7 | ASAC7 | 600 | 45 |
| | Levels | | |
| | − 1 | 0 | 1 |
| $T_f$ (°C) | 500 | 600 | 700 |
| Hold time (min) | 30 | 45 | 60 |

### Preparation of activated carbon

The preparation of the ACs followed the procedures described by Ribas et al. (2014) and Leite et al. (2017): 100.0 g of avocado seed (AS) was milled at diameter < 250 μm; 100.0 g of $ZnCl_2$ and 30.0 mL of water were added and mixed until they form a homogeneous paste (Leite et al. 2017). The resulting paste was placed in a quartz tube reactor inside conventional heating furnace (Sanchis, Porto Alegre, RS, Brazil). The heating treatment was carried out by heating the sample from room temperature until final temperature ($T_f$), according to data of Table 1, and $N_2$ flow (150 mL/min). Then, the system was cooled down, also under $N_2$ atmosphere, until the temperature attain values < 150 °C.

Afterwards, the pyrolysed materials were treated with a 6 mol $L^{-1}$ HCl solution under reflux at 80 °C (Ribas et al. 2014; Saucier et al. 2015; Leite et al. 2017). The resulting activated carbons were labelled according to the experiments performed in the full $2^2$ factorial design as ASAC1 to ASAC7 for experiments from 1 to 7 (see Table 1).

### ASAC characterisation

Nitrogen adsorption isotherms were recorded with a Micrometrics Instrument, TriStar II 3020 at − 196 °C after drying for 3 h at 120 °C under reduced pressure (< 2 mbar) (Umpierres et al. 2017). The specific surface areas were determined from the Brunauer, Emmett and Teller (BET) method (Thommes et al. 2015). Pore size was calculated by the Barrett–Joyner–Halenda (BJH) method from desorption curves (Thommes et al. 2015).

Surface images were observed with a scanning electron microscope (SEM) (TESCAN 3, Sweden) (Lemraski et al. 2017).

The functional groups of the hybrid materials were determined using a Bruker spectrometer and alpha model fourier transform infrared spectroscopy (FTIR). The spectrum was recorded with 64 cumulative scans over the range of 4000–400 $cm^{-1}$ with a resolution of 4 $cm^{-1}$ (Zhang et al. 2017a).

Thermogravimetric analyses (TGA) were obtained on a TA Instruments model SDT Q600 (New Castle, USA) with a heating rate of 20 °C $min^{-1}$ at 100 mL $min^{-1}$ of synthetic air flow. Temperature was varied from 20 to 1000 °C with an acquisition time of 1 point per 5 s using 10.00–15.00 mg of solid (Wang et al. 2017).

For determination of hydrophobicity/hydrophilicity of the surfaces, the ACs were dried in 10-mL beakers at 70 °C for 24 h (dos Reis et al. 2016b; Prenzel et al. 2014). Then, the samples were cooled down in a desiccator before the accurate weight (ca. 0.3 g) of each sample was obtained. Afterwards, the beakers were disposed into capped Erlenmeyer flasks, containing 60 mL of solvent (water or *n*-heptane) inside a temperature-regulated shaker at 25.0 ± 0.1 °C in static condition. The samples were placed in such a way that they were not in contact with the solvent or wall of the Erlenmeyer. After 24 h, the sample was removed from the Erlenmeyer, dried carefully from the outside with laboratory tissues and weighed again. The maximal vapour amount adsorbed on the ACs was obtained by the difference between the final and initial weight and expressed in milligrammes per gramme (dos Reis et al. 2016b; Prenzel et al. 2014). The hydrophobicity/hydrophilicity balances (HI) were calculated as the ratio of

adsorbed *n*-heptane vapour (mg $g^{-1}$) to adsorbed water vapour amount (mg $g^{-1}$).

The $pH_{pzc}$ values were determined through the procedure described in the literature (Prola et al. 2013a). The total acidity and basicity of the ACs were determined using a modified Boehm titration (Goertzen et al. 2010; Thue et al. 2017).

### Chemicals, reagents and solutions

Deionized water was used for preparation of all solutions.

All phenolic compounds and pharmaceuticals used in the adsorption processes were purchased from Sigma-Aldrich (São Paulo, Brazil) and are listed in the Table 2 (Pubchem 2017), and their chemical structures are depicted on Supplementary Fig. 1 and Supplementary Fig. 2.

The solutions used for the experiments of adsorption were 200 mg $L^{-1}$ of pharmaceuticals and 500 mg $L^{-1}$ of phenols that were prepared from stock solutions of 1000 mg $L^{-1}$. The pH of these solutions was 7.0 for the majority of these compounds, with exception of nimesulide (pH 8.5), tetracycline (pH 8.5), 1-naphtol (pH 10.5), 2-naphthol (pH 10.5), bisphenol A (pH 10.5) and thymol (pH 11.5).

### Batch adsorption studies and quality assurance

The batch adsorption processes for the phenolic compounds and pharmaceuticals on seven ASACs materials were performed using 20.00 mL of phenolic (500 mg $L^{-1}$) and pharmaceutical (200 mg $L^{-1}$) solutions at a suitable pH, which were quantitatively transferred to 50.0-mL flat Falcon tubes containing 30.0 mg of ASAC adsorbent (1.5 g $L^{-1}$). The flasks were capped and placed horizontally in a thermostatic reciprocating shaker (25.0 ± 0.1 °C) model Oxy-303T, furnished by Oxylab (Novo Hamburgo, RS, Brazil), using a contact time of 120 min. After the stipulated time, the flasks were removed and centrifuged to separate the adsorbents from the aqueous solutions, and aliquots of 1–5 mL of the supernatants were properly diluted to 10.0–100.0 mL in calibrated flasks using aqueous solution at suitable pH.

The residual solutions of each adsorbate after adsorption were measured using a UV-visible spectrophotometer at their respective wavelengths, and the adsorption capacity ($q_e$) was determined using the relation shown in Eq. (1).

$$q = \frac{(C_0 - C_f)}{m} V \quad (1)$$

where $q$ (mg $g^{-1}$) is the amount of the used adsorbate adsorbed per unit adsorbent; $C_0$ and $C_f$ (mg/L) are the initial and equilibrium liquid phase concentrations, respectively; $V$ (L) is the volume of the adsorbate solution; and $m$ (g) is the adsorbent amount.

All of the experiments were carried out in triplicate to ensure reproducibility, reliability and accuracy of data. The relative standard deviations of all measurements were < 4.5%. Blanks were run in parallel and corrected when necessary (Barbosa-Jr et al. 2000).

The solutions of adsorbates were stored in glass bottles, which were cleaned by immersing in 1.4 mol $L^{-1}$ $HNO_3$ for 24 h (Lima et al. 2001), rinsing with deionized water, drying and keeping them in cabinets.

Adsorbate solutions (between 2.00–100.0 mg $L^{-1}$), in parallel with a blank, were used for linear analytical calibration. The calibration curves were performed on the UV-Win software of the T90+ PG Instruments spectrophotometer. All of the analytical measurements were repeated thrice, and the precisions of the standards were better than 5.0% ($n = 3$) (Lima et al. 2000). The adsorbate solutions (15.0 mg $L^{-1}$) were used as quality control after every five measurements to ensure accuracy of the solutions (Barbosa-Jr et al. 1999).

## Results and discussion

### SEM analysis

Analysis such as SEM, in view of its ability to directly view the surface of activated carbons at high magnification, has demonstrated enormous potential for use in the study and characterisation of activated carbons (Thue et al. 2016, 2017; Lemraski et al. 2017). SEM was used to observe the physical surface of the all ASAC samples (see Fig. 1). Such images show that the activation stage produced carbon surfaces which were very irregular in relation to its format and present high roughness. At the amplification of × 1000 (at micrometric scale), it is not possible to distinguish the ASAC samples from each other.

### Specific surface area and porosity

Specific surface area and porosity are two important physical properties of a material that impact its quality and utility for a certain application, especially for adsorption process. These physical characteristics are important because they are deeply related to adsorptive capacity of the materials (Thue et al. 2016, 2017; dos Reis et al. 2016a, c). Many works have addressed that the success in the application of adsorbents is closely linked with specific surface area and porosity characteristics of these adsorbents (Leite et al. 2017; Thue et al. 2016, 2017; Lin et al. 2017c).

The physical features of the avocado seed activated carbons made by different pyrolysis conditions are shown in Table 3. By analysing Table 3, it is easy to see that the textural properties of the obtained activated carbons differ in relation to its pyrolysis conditions.

**Table 2** Physico-chemical properties of the molecules

| Compound | Molecular formula | $\lambda_{max}$ (nm) | Molecular weight (g $mol^{-1}$) | Solubility in water (g $L^{-1}$)[a] | Van der Waals surface area ($A^2$, pH 7.0)[b] | Polar surface area ($A^2$, pH 7.0)[b] | Van der Waals volume ($A^3$)[b] | Polar surface area/Van der Waals surface area ratio | Log $P$[b] |
|---|---|---|---|---|---|---|---|---|---|
| Pharmaceuticals | | | | | | | | | |
| Amoxicillin | $C_{16}H_{19}N_3O_5S$ | 227.0 | 365.404 | 3.430 | 476.14 | 162.71 | 307.13 | 0.3417 | 0.87 |
| Caffeine | $C_8H_{10}N_4O_2$ | 273.0 | 194.194 | 21.60 | 269.07 | 58.44 | 164.20 | 0.2172 | − 0.07 |
| Captopril | $C_9H_{15}NO_3S$ | 200.0 | 217.283 | 4.52 | 318.05 | 99.24 | 196.51 | 0.3120 | 0.34 |
| Enalapril | $C_{20}H_{28}N_2O_5$ | 270.5 | 376.453 | 16.40 | 591.12 | 98.77 | 357.31 | 0.1671 | 0.07 |
| Meloxicam | $C_{14}H_{13}N_3O_4S_2$ | 359.0 | 351.395 | 15.40 (pH 7.0)[b] | 421.52 | 139.05 | 275.99 | 0.3299 | 3.54 |
| Nimesulide | $C_{13}H_{12}N_2O_5S$ | 392.5 | 308.308 | 2.19 (pH 8.5)[b] | 407.92 | 104.12 | 249.17 | 0.2552 | 2.60 |
| Paracetamol | $C_8H_9NO_2$ | 243.0 | 151.165 | 14.00 | 251.37 | 49.33 | 159.08 | 0.1962 | 0.46 |
| Propanolol | $C_{16}H_{21}NO_2$ | 289.5 | 259.349 | 24.09 (pH 7.0)[b] | 430.03 | 46.07 | 257.37 | 0.1071 | 3.48 |
| Sodium diclofenac | $C_{14}H_{10}Cl_2NO_2Na$ | 275.5 | 318.129 | 6.02 (pH 7.0)[b] | 359.64 | 52.16 | 234.43 | 0.1450 | − 2.31 |
| Tetracycline | $C_{13}H_{12}N_2O_5S$ | 357.0 | 308.308 | 2.19 (pH 8.5)[b] | 407.92 | 104.12 | 249.17 | 0.2552 | − 1.37 |
| Phenols | | | | | | | | | |
| 1-Naphthol | $C_{10}H_8O$ | 292.5 | 144.173 | 1.79 (pH 10.5)[b] | 209.50 | 20.23 | 133.72 | 0.0966 | 2.85 |
| 2-Naphthol | $C_{10}H_8O$ | 273.5 | 144.173 | 1.25 (pH 10.5)[b] | 209.70 | 20.23 | 133.65 | 0.0965 | 2.70 |
| 2-Aminophenol | $C_6H_7NO$ | 283.0 | 109.128 | 20.00 | 161.26 | 46.25 | 101.48 | 0.2868 | 0.62 |
| 3-Aminophenol | $C_6H_7NO$ | 281.0 | 109.128 | 19.39 (pH 7.0)[b] | 161.99 | 46.25 | 101.50 | 0.2855 | 0.21 |
| 2-Chlorophenol | $C_6H_5ClO$ | 273.5 | 128.555 | 2.75 (pH 7.0)[b] | 162.88 | 20.23 | 104.48 | 0.1242 | 2.15 |
| 2-Nitrophenol | $C_6H_5NO_3$ | 278.0 | 139.110 | 2.10 | 181.86 | 66.20 | 113.52 | 0.3640 | 1.79 |
| 4-Nitrophenol | $C_6H_5NO_3$ | 226.0 | 139.110 | 11.60 | 185.14 | 63.37 | 113.43 | 0.3423 | 1.91 |
| Pyrocatechol | $C_6H_6O_2$ | 275.0 | 110.112 | 33.24 | 158.06 | 40.46 | 99.01 | 0.2560 | 0.88 |
| Resorcinol | $C_6H_6O_2$ | 273.0 | 110.112 | 33.42 | 158.57 | 40.46 | 99.03 | 0.2552 | 0.80 |
| Hydroquinone | $C_6H_6O_2$ | 288.0 | 110.112 | 6.72 | 158.58 | 40.46 | 99.04 | 0.2551 | 0.59 |
| *o*-Cresol | $C_7H_8O$ | 270.0 | 108.140 | 6.67 | 179.02 | 20.23 | 107.37 | 0.1130 | 1.95 |
| *m*-Cresol | $C_7H_8O$ | 271.0 | 108.140 | 3.94 | 179.31 | 20.23 | 107.32 | 0.1128 | 1.96 |
| 4-Methoxyphenol | $C_7H_8O_2$ | 287.5 | 124.139 | 13.24 | 195.05 | 29.46 | 116.49 | 0.1510 | 1.58 |
| Bisphenol A | $C_{15}H_{16}O_2$ | 276.0 | 228.291 | 1.96 (pH 10.5)[b] | 359.75 | 40.46 | 221.44 | 0.1125 | 3.32 |
| Thymol | $C_{10}H_{14}O$ | 273.0 | 150.221 | 2.39 (pH 11.5)[b] | 271.49 | 20.23 | 158.40 | 0.0745 | 3.30 |

[a] Pubchem: https://pubchem.ncbi.nlm.nih.gov/. Site visited on September 27, 2017

[b] Chemical properties were calculated using the plug-in of Marvin Sketch 17.16.0 (www.chemaxon.com 2017)

For the $S_{BET}$, it should be noted that their values are high-presenting values ranging from 1122 to 1584 $m^2$ $g^{-1}$ (see Table 3). The high values of $S_{BET}$ might implicate in high uptakes of adsorbates by ASACs (Lin et al. 2017c; Thue et al. 2016, 2017). Therefore, it should be pointed out that avocado seed is an excellent precursor for preparation of highly porous activated carbons.

Other parameters that are useful for analysis of the textural properties of these ASAC materials are micropore area and external surface area and total, micropore and mesopore volumes. As can be seen in Table 3, all these parameters have followed the same $S_{BET}$ trend, as earlier observed for other activated carbons (Thue et al. 2016, 2017; Ahmed et al. 2017). It is noted that the samples pyrolysed at 500 °C reached higher textural parameter values compared with those samples pyrolysed at 700 °C.

It is also valuable to classify the activated carbons by their relationship between microporosity and

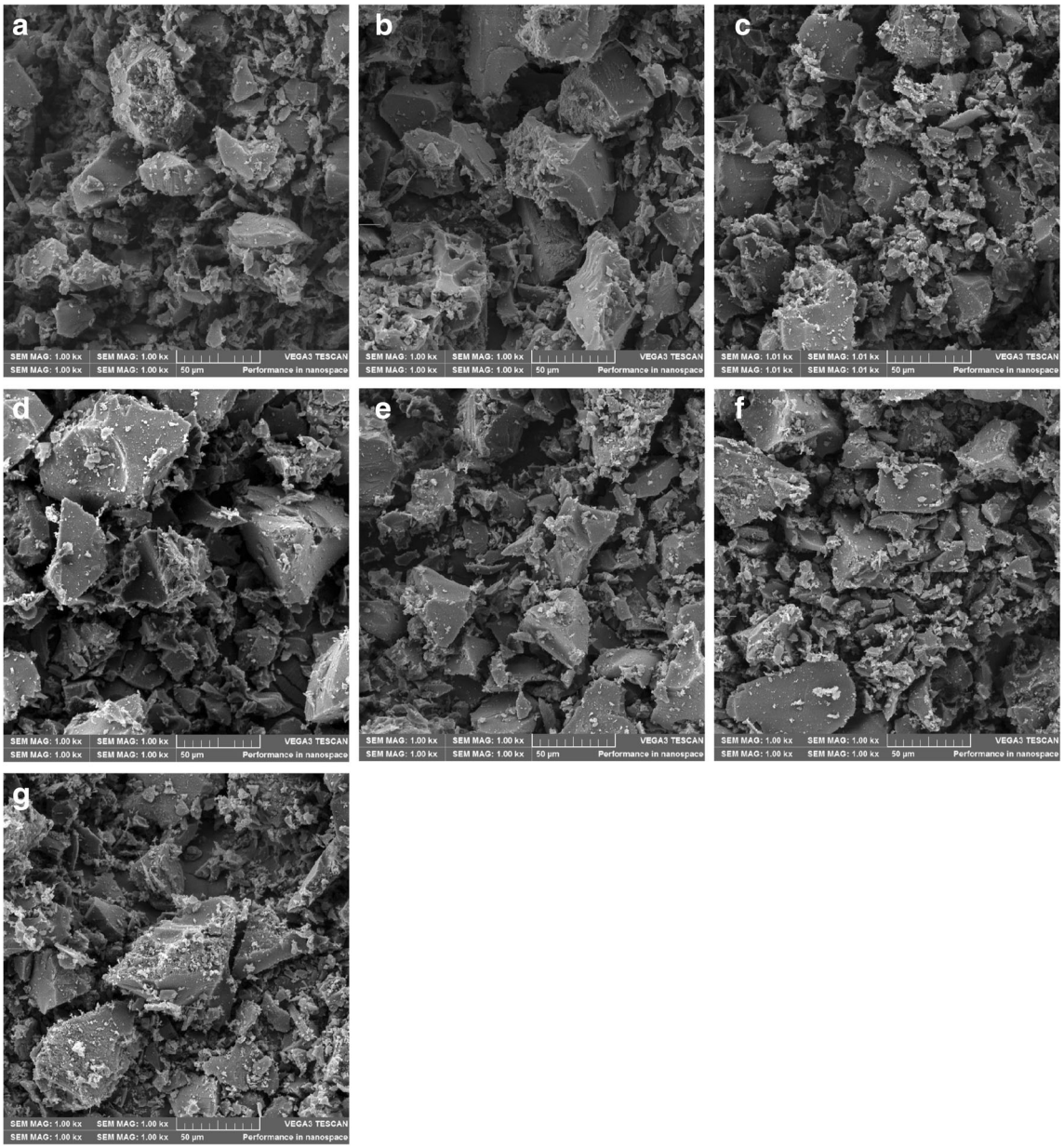


**Fig. 1** SEM images of avocado seed activated carbon (ASACs). **a** ASAC1. **b** ASAC2. **c** ASAC3. **d** ASAC4. **e** ASAC5. **f** ASAC6. **g** ASAC7. All images correspond to a magnification of × 1000

**Table 3** Textural properties of avocado seed activated carbons

| Sample | BET surface area ($m^2\ g^{-1}$) | *t*-plot micropore area ($m^2\ g^{-1}$) | *t*-plot extern. surface area ($m^2\ g^{-1}$) | Total pore volume ($cm^3\ g^{-1}$) | *t*-plot micropore volume ($cm^3\ g^{-1}$) | Mesopore volume ($cm^3\ g^{-1}$) |
|---|---|---|---|---|---|---|
| ASAC1 | 1584 | 360 | 1224 | 0.8469 | 0.1563 | 0.6906 |
| ASAC2 | 1230 | 201 | 1029 | 0.6685 | 0.0838 | 0.5847 |
| ASAC3 | 1370 | 263 | 1107 | 0.7664 | 0.1120 | 0.6544 |
| ASAC4 | 1122 | 284 | 838 | 0.6002 | 0.1249 | 0.4753 |
| ASAC5 | 1343 | 316 | 1027 | 0.7354 | 0.1354 | 0.6000 |
| ASAC6 | 1300 | 250 | 1050 | 0.7248 | 0.1261 | 0.5987 |
| ASAC7 | 1310 | 237 | 1073 | 0.7232 | 0.1376 | 0.5856 |

mesoporosity. Therefore, the volumes of mesopores were divided by the total pore volume and the values were multiplied by 100%. The percentages of mesopores obtained were 81.54, 87.46, 85.39, 79.19, 81.59, 82.60 and 80.97% for ASAC1, ASAC2, ASAC3, ASAC4, ASAC5, ASAC6 and ASAC7, respectively. Based on these values, clearly, it is seen that all of the obtained activated carbons are predominantly mesoporous materials which could facilitate their uses in adsorption processes, in which adsorbate molecules diffuses through the pores of the ASACs (Leite et al. 2017; Thue et al. 2016, 2017).

Observing the values of specific surface area and total pore volume of the obtained ASAC adsorbents (Table 3), the values of surface area are ranging from 1122 to 1584 $m^2\ g^{-1}$ and for total pore volume ranging from 0.6002 to 0.8469 $cm^3\ g^{-1}$, which are very good values when compared with data already published in the literature. Rovani et al. (2016) produced activated carbon from agro-industrial wastes such as coffee, wood and apple pomace wastes; the highest surface area was achieved by apple pomace wastes with a specific area of 176.4–209.9 $m^2\ g^{-1}$ and total pore volume of 0.2571 to 0.2822 g $cm^{-3}$; Dos Reis et al. (2016a) produced activated carbon from sewage sludge obtaining specific surface area ranging from 387.7 to 679.3 $m^2\ g^{-1}$ and total pore volume ranging from 0.379 to 0.690 g $cm^{-3}$; Calvete et al. (2010) produced activated carbon from pinon wastes and obtained surface area of 1035 to 1425 $m^2\ g^{-1}$ and total pore volumes ranging from 0.43 to 0.50 g $cm^{-3}$; Ahmed et al. (2017) produced activated carbon from human hair and obtained surface area of 1505 $m^2\ g^{-1}$ and total pore volume of 0.798 g $cm^{-3}$. Based on these data, it can be inferred that the ASAC activated carbons presented higher surface area and higher total pore volume, which are good characteristics for adsorption of different adsorbates (Thue et al. 2016, 2017).

## Fourier transform infrared spectroscopy, point of zero charge, total acidity and basicity (Boehm titration) and hydrophobicity index

FTIR analysis contributes in the identification of functional surface groups present on a solid surface which may contribute for explaining the adsorption of adsorbate molecules onto the carbon surfaces (Ribas et al., 2014; Saucier et al. 2015; Thue et al. 2016, 2017). The FTIR spectra of all ASACs are displayed in Fig. 2. Although some differences in the spectra of ASACs can be seen, it seems that the different conditions in the pyrolysis process did not cause large differences in the spectra of ASACs which presented almost the same group of vibrational FTIR bands, such as the following: The band at 3443–3419 $cm^{-1}$ is due to the OH stretching vibrations from the intermolecular hydrogen bonding (Calvete et al. 2010; Leite et al. 2017; Thue et al. 2016); bands at 2920–2924 and 2853–2858 $cm^{-1}$ are due to the asymmetric and symmetric C–H stretching, respectively (Prola et al. 2013a, b); a small shoulder at 1736–1708 $cm^{-1}$ could assigned to C=O stretching of carboxylic acids (Ribas et al. 2014;); that at 1614–1630 $cm^{-1}$ is due to the asymmetric stretching in of carboxylates (O=C=O) (Thue et al. 2016, 2017); and those at 1409–1410 and 1460 $cm^{-1}$ may be assigned to the aromatic ring mode (Leite et al. 2017; Thue et al. 2016). The bands at 1262–1163 and 1030–1040 $cm^{-1}$ could be assigned to C–O stretching of phenols and alcohols, respectively, and the band at 799–806 $cm^{-1}$ could be assigned to C–H out-of-plane bending in the aromatic rings (Leite et al. 2017; Thue et al. 2016). The most important functional groups present in all ACs include (i) O–H likely from alcohols and phenols, (ii) aromatic rings, (iii) C=O likely from carboxylic acids and esters and (iv) CH from aromatic and aliphatic compounds.

The surface chemistry and functionality of a solid material (specially a functional material such carbon material) are determined by the presence of basic and acidic groups on its surface. The $pH_{pzc}$ is the pH at which the surface of an adsorbent is globally neutral, i.e. contains as much positively charged as negatively charged surface functions. Below this value, the surface is positively charged, making it able to attract anions; beyond this value, it is negatively charged which would attract cations.

It can be seen from Table 4 that the $pH_{pzc}$ values of all samples are between 6.11 and 6.80. These values of $pH_{pzc}$ reveal that the surfaces of these ASACs are close to neutrality; however, it reveals that there are a small excess of acidic groups in relation to basic groups.

The total acidity and total basicity of the ASACs were determined using modified Boehm titration (Goertzen et al. 2010; Thue et al. 2017); see Table 4. This method was preferred in relation to fractionated acidic groups (carboxylic acids, phenolic, lactonic) because the $CO_2$ generated with the use of carbonate and hydrogen carbonate in the aqueous solution leads to wrong results of these groups, which are usually neglected by the majority of authors, who use standard coloured indicator to detect the end point of the titration (Goertzen et al. 2010). It is also observed that the total amount of acidic groups present on the ASAC samples is a little bit higher than that of the basic groups, and this result is consistent with the values of $pH_{pzc}$ reported earlier (Table 4). Samples with higher amount of acidic groups presented lower values of $pH_{pzc}$. Therefore, the values of $pH_{pzc}$ are in complete agreement with the total amounts of acidic and basic groups present in the activated carbon samples.

In relation to the polarity of the surface of the obtained ASAC adsorbents, it was also observed that samples with higher total amount of functional groups (acidic and basic groups) presented lower values of HI (see Table 4). The HI values were calculated as the ratio of the amount of adsorbed *n*-heptane vapour (mg $g^{-1}$) by the ASAC samples divided by

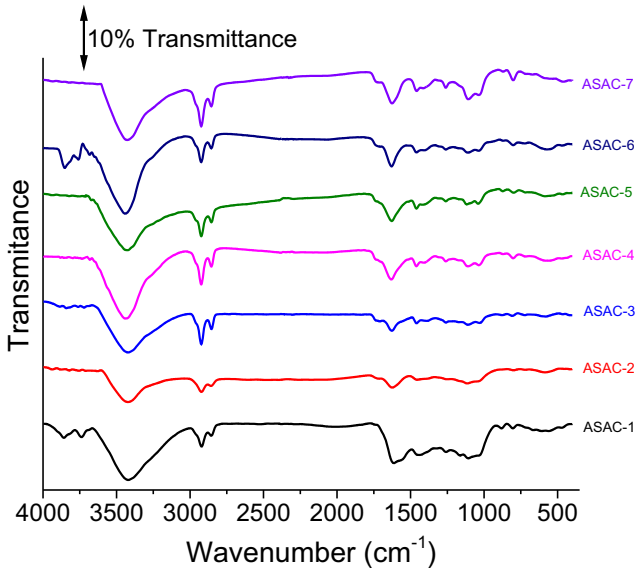


**Fig. 2** FTIR spectra of ASACs

the amount of adsorbed water vapour (mg $g^{-1}$) by the carbon samples (dos Reis et al. 2016b; Prenzel et al. 2014). It is observed that all ASAC surfaces are predominantly hydrophilic in nature (see Table 4), since all HI values are lower than 1.00.

It should be highlighted that the values of $pH_{pzc}$, total amount of functional groups and HI are completely in agreement, reinforcing that these results should be correct.

The presences of hydrophilic groups on ASAC surfaces are related to H– bonding and oxygen groups that are present on the ASAC surfaces (see Fig. 2). Taking into account these set of results presented until here, it differentiates the better pyrolysis conditions to be carried out, in order to obtain activated carbons with higher sorption capacity for removal of organic emerging contaminants. Therefore, it is necessary to use a statistical tool, to differentiate the textural, functional, polarities and surface acidity of activated carbon samples obtained from the conventional pyrolysis of avocado seed which will be presented in the next section.

## Evaluation of the influence variables by statistical analysis

When analysing the effects of multiple variables in an experiment, it is useful to see the normal probability plots of the standardized effects at a given probability level ($p = 0.05$, in this case) to verify what is the variable that has the main effect over a determined response, as well as if the variation of a given parameter will increase or decrease the responses and also it is possible to detect if there are some synergistic or antagonistic effect of varying two or more variables simultaneously. Based on that, in this study, normal probability plots of the standardized effects at $p = 0.05$ for the responses, surface area (Supplementary Fig. 3A), total volume of pores (Supplementary Fig. 3B), total functional groups (Supplementary Fig. 3C) and HI (Supplementary Fig. 3D) for producing activated carbons from avocado seed using the experimental conditions are depicted on Table 1. These graphs could be divided in two regions: at the left of zero standardized effect, where the factors and their interactions presented negative coefficients, and at the right of zero standardized effect where the factors presented positive coefficients. All these factors and interactions which were represented as a square were significant figures, and they were out of the central line that crosses the zero value at the abscissa at 50%. The effects positioned in this line were represented by a circle and correspond to the estimate of errors of the effects, being not significant (Bruns et al. 2006; Montgomery 2017). As the probability level was established at 95% of confidence level ($p = 0.05$), all factors and interactions with values of probability lower than 0.05 are significant (see Supplementary Table 1) and all parameters or interactions of two factors with probability > 0.05 are not significant. Also, the contribution of each factor and its interaction in the overall responses were also given (see Supplementary Table 1).

For the response of surface area ($S_{BET}$), it was observed that the parameters' final temperature (A) and time of holding the pyrolysis at the final temperature (B) presented both negative coefficients and for this response, there is no interaction of the

**Table 4** Chemical surface properties of avocado seed activated carbons

| Sample | $pH_{pzc}$ | Total acidity (mmol $g^{-1}$) | Total basicity (mmol $g^{-1}$) | Total of functional groups (mmol $g^{-1}$) | HI |
|---|---|---|---|---|---|
| ASAC1 | 6.11 | 0.2950 | 0.1885 | 0.4835 | 0.7884 |
| ASAC2 | 6.80 | 0.2054 | 0.1568 | 0.3622 | 0.8750 |
| ASAC3 | 6.32 | 0.2831 | 0.1475 | 0.4306 | 0.7889 |
| ASAC4 | 6.85 | 0.1907 | 0.1590 | 0.3497 | 0.9146 |
| ASAC5 | 6.48 | 0.2145 | 0.1547 | 0.3692 | 0.8047 |
| ASAC6 | 6.55 | 0.2245 | 0.1547 | 0.3792 | 0.8045 |
| ASAC7 | 6.52 | 0.2137 | 0.1608 | 0.3745 | 0.8041 |

*HI* amount of adsorbed vapour of *n*-heptane (mg $g^{-1}$) divided by amount of adsorbed vapour of water (mg $g^{-1}$)

two factors. The contribution of the parameter temperature of pyrolysis corresponds to 77.90% of the overall response (in standardized effects), followed by the time of holding pyrolysis (20.71%). The contributions of interaction of two factors (A × B), central point and error were 0.27, 0.24 and 0.88%, respectively. Based on these results (Supplementary Fig. 3A and Supplementary Table 1A), when the temperature of pyrolysis of avocado seed passes from 500 to 700 °C, a decrease in the surface area will be observed. Also, the increase of time of pyrolysis, from 30 to 60 min, also led to a decrease in surface area. The effect of increase in temperature of pyrolysis and time of holding temperature on the surface area was already reported in the literature by Botomé et al. (2017), and the authors also observed a decrease in the surface area.

For the response total pore volume, all the factors (A and B) and the interactions of two factors (A × B) were significant (see Supplementary Fig. 3B and Supplementary Table 1B). Also, it was observed that increases in the temperature of pyrolysis (A) and holding time at the final temperature (B) as well as the interaction A × B presented negative coefficients, meaning that its increases in their values lead to a decrease in the total pore volume. The contributions of each factor on the overall response were 71.28% (A), 16.40% (B), 5.23% (A × B), 6.96% (central point) and only 0.13% (pure error). Considering that there was significant central point in the response total pore volume, it is possible to highlight that a curvature occurred for this response. Also, interactions of temperature of pyrolysis and time of holding at final temperature also decreased the total pore volume (negative coefficient). Although these two parameters were observed (A × B and central point), the final temperature of pyrolysis (A) is the factor that contributes the most with the total pore volume.

There is a direct relationship between surface area and total pore volume of an activated carbon (Thue et al. 2016, 2017). As the total surface area of ASACs increases, it would lead to increases in the total pore volume. The increase in temperature and holding time at final temperature led to decreases in the surface area (Supplementary Fig. 3A) and total pore volume (Supplementary Fig. 3B).

For the response of total functional groups present on the surface of ASACs, an interesting effect of the parameters was obtained. The temperature of pyrolysis (A) and holding time (B) present negative coefficients; on the other hand, the interactions of temperature of pyrolysis multiplied by holding time (A × B) present a positive coefficient. In addition, the magnitude of A × B is very close to that of A (see Supplementary Table 1C). The overall response (total amount of functional groups) follows a decreasing order, temperature (41.42%), holding time (21.37%), interaction A × B (20.82%), central point (16.39%) and pure error (0.00%). Again, the presence of a central point indicates the curvature when the temperature and the holding time are increased from 500 to 700 °C and 30 to 60 min, respectively. The increase in temperature leads to a decrease in the total functions present on the surface of activated carbons as expected (dos Reis et al. 2016a, c). The increase in temperature during the pyrolysis leads to the elimination of the most volatile organic groups of the pyrolysed lignocellulosic material (Saucier et al. 2015) that will render low contents of organic groups onto the surface of ASAC samples. Also, the increase in the holding time will increase the releases of volatile organic groups (dos Reis et al. 2016a, c). However, the synergistic effect of temperature of pyrolysis multiplied by the holding time (A × B) is not expected in the univariate analysis, and just this result justifies the $2^2$ full-factorial design with three central points carried out in this work.

The hydrophobic/hydrophilic ratio (HI) was the fourth response explored in this work. Contrary to all the responses shown until now, all the coefficients presented positive values (see Supplementary Fig. 3D and Supplementary Table 1D). The increase in the temperature of pyrolysis as well as the holding time of the final temperature of pyrolysis led to increase in the HI values, which means that the ASAC surfaces of the carbon adsorbents became less hydrophilic (since all values of HI are lower than 1.00). This achievement is compatible with total organic functional groups. The increase in temperature leads to releases of oxygen functional groups, and therefore, the carbon surfaces become more hydrophobic (dos Reis et al. 2016b; Prenzel et al. 2014). The overall HI response for the factorial design followed a decreasing order, temperature of pyrolysis (36.47%), holding time (24.01%), the interaction of two factors temperature of pyrolysis multiplied by holding time (24.00%) and central point (15.52%).

Based on the DOE of the four responses studied, the following could be drawn:

- For obtaining activated carbons with higher surface area and higher total pore volumes, it would be better to use lower pyrolysis temperatures and holding times;
- For obtaining activated carbons with higher number of total functional groups, it would be better also to use lower pyrolysis temperatures and holding times.

However, it should be mentioned that higher surface area, higher total pore volume and higher functional groups are not a guarantee that the activated carbon will be a good adsorbent for removal of emerging organic contaminants from aqueous solutions, because the adsorption does not take into account the physical characteristics of the adsorbent (higher surface area, higher total pore volume). It also considers the chemical nature of adsorbate and adsorbent and the chemical composition of the medium (Lima et al. 2015).

## Adsorption of emerging pollutants

Among the different types of organic pollutants in wastewater, phenolic and several pharmaceutical compounds are considered as priority pollutants since they cause several issues for the living organisms, even at very low concentrations. Removal of these emerging compounds by adsorption onto activated carbon is one of the most applied methods for treating polluted waters. In this work, avocado seed was used as raw material for preparation of activated carbons and they were used for uptake of 15 phenolic compounds and 10 pharmaceuticals in aqueous solutions as shown in Table 5. The ASACs exhibited very high adsorption capacity for all organic emerging contaminants.

It is well-known in the literature that the adsorption characteristics of different phenolic and pharmaceutical compounds are influenced by their physicochemical properties, such as water solubility and octanol–water partition coefficients (dos Reis et al. 2017, Thue et al. 2016, 2017; Yang et al. 2017). However, in this study, the affinity of each organic emerging contaminant compared with others does not follow a logical pattern with respect to their physical chemical properties, reported in Table 2, in order to differentiate the reason for the differences on sorption capacities of different emerging organic contaminants. We tried to make some correlation of amount adsorbed of the organic compound with its molecular weight, its Van der Waals and polar surface areas, its ratio of polar surface area divided by the Van der Waals surface area, its Van der Waals volume and its Log *P*. However, all these parameters did not follow a logical pattern to explain why the ASACs presented differences in the sorption capacity for these 25 emerging organic contaminants. Therefore, the statistical analysis, described below, helped to understand these differences.

The results shown in Table 5 suggest that the ASACs could be successfully employed for removal of organic emerging compounds from aqueous solutions. The reasons for this could be several. However, what better explains the efficiency in the removal of such adsorbates is the mechanism of adsorption. To better understand the possible mechanisms that might play key roles in phenolic compound adsorption on ASACs, some mechanisms, such as $\pi$–$\pi$ interactions, dispersion interactions, electron donor–acceptor and hydrogen bonds (dos Reis et al. 2016c; Thue et al. 2016), are proposed.

In the ASACs, surfaces are expected to contain large amounts of polar groups such as –OH, –COO, –O and –NH, (as can be seen in the FTIR analysis) and exhibit mostly polar (hydrophilic) behaviour.

The organic emerging contaminant adsorption on ASACs could also be determined by $\pi$–$\pi$ interactions (between the $\pi$ electrons present in the rings of phenols with the $\pi$ electrons of the aromatic rings present on ASACs) and "donor–acceptor complex" formation between the surface carbonyl groups (electron donors) and the aromatic ring of phenol acting as the acceptor.

It is clearly seen that although the ASAC-1 has the highest $S_{BET}$ and total pore volume (1584 $m^2\ g^{-1}$ and 0.8469 $cm^3\ g^{-1}$, respectively) among the others, it does not present the highest uptake, which suggests that the adsorption of emerging pollutants such phenols and pharmaceuticals is not totally influenced by physical features of the ASACs (see Table 5). The differences between the values of $q$ might also be linked by the physical–chemical properties of the emerging pollutants; however, no logical pattern was followed as can be seen by the physical–chemical properties shown in Table 2 as well as in the Supplementary Fig. 1 and Supplementary Fig. 2.

However, observing Table 5 as well as the results of Table 4, the decreasing sorption capacity of the ASAC for all organic emerging contaminants was as follows: ASAC4 > ASAC2 > ASAC7 ≈ ASAC6 ≈ ASAC5 > ASAC3 > ASAC1. This order is exactly the opposite order of total functional groups, whose decreasing order was ASAC1 > ASAC3 > ASAC6 ≈ ASAC7 ≈ ASAC5 > ASAC2 > ASAC4. Also, the sorption decreasing order of ASACs also agrees with that of the HI ratio, whose decreasing order is ASAC4 > ASAC2 > ASAC5 ≈ ASAC6 ≈ ASAC7 > ASAC3 > ASAC1. Based on these results, it can be concluded that the sorption capacity of the emerging organic contaminants decreased as the number of total basic and acidic groups increased, and the sorption capacity also increased with the increase in HI ratio, and this analysis was observed based on the statistical results of the factorial design.

Considering that all activated carbons prepared in this work presented surface area higher than 1000 $m^2\ g^{-1}$ (see Table 3) and considering that a pyrolysis temperature of avocado seed carried out at 700 °C led to a decrease in functional groups (acidic and basic functional groups) onto the surface of activated carbon, which resulted in the most hydrophobic surface, when compared with the activated carbons (see Table 4), whose final pyrolysis temperature was 500 °C, it could be stated that for adsorption of 25 emerging contaminants, the best activated carbon was ASAC4. However, all other activated carbons also could be successfully employed for adsorption of organic compounds from aqueous solutions.

## Comparison of adsorption capacities of different adsorbents

In order to compare the effectiveness of the avocado activated carbons for removal of phenolic compounds, Table 6 brings some results of some works reported in literature in relation to adsorption of some phenolic compounds and pharmaceuticals over many types of ACs. The results found in literature might enable a comparison analysis about the effectiveness the avocado ACs prepared in this work (see Table 5) with many other adsorbents.

**Table 5** Sorption capacity of 25 emerging organic contaminants

| | Sorption capacity (mg $g^{-1}$) | | | | |
|---|---|---|---|---|---|
| | Amoxicillin | Caffeine | Captopril | Enalapril | Meloxicam |
| ASAC1 | 71.94 | 116.86 | 122.58 | 99.56 | 180.26 |
| ASAC2 | 109.97 | 129.43 | 131.58 | 119.08 | 199.87 |
| ASAC3 | 74.52 | 119.56 | 123.25 | 100.32 | 182.36 |
| ASAC4 | 110.00 | 131.85 | 132.01 | 121.74 | 201.36 |
| ASAC5 | 95.85 | 126.15 | 129.58 | 110.12 | 196.25 |
| ASAC6 | 97.83 | 127.12 | 127.58 | 110.68 | 195.25 |
| ASAC7 | 94.56 | 125.58 | 128.25 | 112.36 | 194.25 |
| | Nimesulide | Paracetamol | Propanolol | Sodium diclofenac | Tetracycline |
| ASAC1 | 117.56 | 95.56 | 69.25 | 121.25 | 188.52 |
| ASAC2 | 133.85 | 121.69 | 102.58 | 131.05 | 197.85 |
| ASAC3 | 119.25 | 105.21 | 71.25 | 124.25 | 191.25 |
| ASAC4 | 134.01 | 122.56 | 104.03 | 132.52 | 200.36 |
| ASAC5 | 127.25 | 99.95 | 99.62 | 126.89 | 196.52 |
| ASAC6 | 126.36 | 98.65 | 98.91 | 127.58 | 198.52 |
| ASAC7 | 127.52 | 97.25 | 99.67 | 129.99 | 197.25 |
| | 2-Aminophenol | 3-Aminophenol | 1-Naphtol | 2-Naphtol | Thymol |
| ASAC1 | 297.36 | 147.25 | 301.58 | 270.69 | 278.52 |
| ASAC2 | 330.87 | 268.25 | 331.39 | 317.73 | 301.50 |
| ASAC3 | 299.34 | 149.71 | 305.52 | 275.58 | 280.56 |
| ASAC4 | 331.08 | 270.58 | 332.58 | 319.29 | 302.25 |
| ASAC5 | 325.24 | 187.69 | 318.25 | 305.25 | 290.52 |
| ASAC6 | 327.58 | 189.07 | 317.25 | 306.53 | 291.52 |
| ASAC7 | 329.32 | 184.69 | 316.54 | 304.26 | 292.36 |
| | 2-Nitrophenol | 4-Nitrophenol | Cathecol | Resorcinol | Hydroquinone |
| ASAC1 | 275.35 | 238.37 | 141.25 | 99.52 | 130.25 |
| ASAC2 | 306.58 | 261.64 | 229.58 | 170.53 | 305.05 |
| ASAC3 | 277.56 | 242.62 | 142.21 | 101.95 | 133.78 |
| ASAC4 | 307.43 | 266.03 | 231.71 | 172.91 | 307.98 |
| ASAC5 | 292.54 | 264.86 | 181.02 | 142.35 | 226.75 |
| ASAC6 | 295.24 | 267.01 | 183.88 | 145.54 | 224.56 |
| ASAC7 | 294.61 | 265.25 | 180.48 | 144.25 | 226.45 |
| | 2-Chlorophenol | *o*-Cresol | *m*-Cresol | 4-Methoxyphenol | Bisphenol A |
| ASAC1 | 202.38 | 148.24 | 135.58 | 197.35 | 314.56 |
| ASAC2 | 239.98 | 201.57 | 182.59 | 272.58 | 327.25 |
| ASAC3 | 204.56 | 149.58 | 139.25 | 201.55 | 315.45 |
| ASAC4 | 241.25 | 202.58 | 183.47 | 277.17 | 325.07 |
| ASAC5 | 240.79 | 178.25 | 177.25 | 240.03 | 319.56 |
| ASAC6 | 242.05 | 177.64 | 181.91 | 243.81 | 318.47 |
| ASAC7 | 240.69 | 175.26 | 175.25 | 242.69 | 317.52 |

As can be seen in Tables 5 and 6, the adsorbent materials proposed in this current work presented very good adsorption capacities when compared with other adsorbents reported in the literature. It is also highlighted that avocado ACs also presented higher adsorption capacities when compared with other adsorbents reported in the literature. However, these results are very important because they highlight the excellent performance of avocado ACs on the removal of several

**Table 6** Maximum sorption capacities of different adsorbents used for removal of various pharmaceuticals and phenolic compounds

| Adsorbent | Phenolic compounds | $Q$ (mg $g^{-1}$) | References |
|---|---|---|---|
| Hyacinth AC | 2-Nitrophenol | 47.62 | Isichei and Okieimen (2014) |
| Mesoporous carbon | Resorcinol | 37 | Shou et al. (2016) |
| Mesoporous silica | Resorcinol | 39.2 | Guo et al. (2013) |
| Coal AC | 3-Aminophenol | 110 | Petrova et al. (2011) |
| Mesoporous carbons | Resorcinol | 40.6 | Ren et al. (2016) |
| AC waste rubber | *p*-Cresol | 250 | Gupta al. (2014) |
| Eggshells carbons | Phenol | 192 | Giraldo and Moreno-Piraján (2014) |
| Activated carbon | 2-Chlorophenol | 549.5 | Strachowski and Bystrzejewski (2016) |
| Aminated AC | Phenol | 227.27 | Yang et al. (2014) |
| Granular AC | Catechol | 100 | Suresh et al. (2011) |
| Granular AC | Resorcinol | 113 | Suresh et al. (2011) |
| Sludge AC | Resorcinol | 406.9 | Dos Reis et al. (2017) |
| Sludge AC | 3-Aminophenol | 454.5 | Dos Reis et al. (2017) |
| Sludge AC | Hydroquinone | 117.1 | Dos Reis et al. (2017) |
| Sludge AC | | | Dos Reis et al. (2017) |
| | Pharmaceuticals | | |
| Sludge AC | Diclofenac | 156.7 | Dos Reis et al. (2016b) |
| Sludge AC | Nimesulide | 66.4 | Dos Reis et al. (2016b) |
| Cotton waste AC | Tetracycline | 109 | Boudrahema et al. (2017) |
| Cotton waste AC | Paracetamol | 105 | Boudrahema et al. (2017) |
| Pineapple leaves AC | Caffeine | 155.5 | Beltrame et al. (2018) |
| Olive stone AC | Diclofenac | 3.104 | Larous and Meniai (2016) |
| Cocoa shell AC | Nimesulide | 74.81 | Saucier et al. (2015) |
| Human hair AC | Tetracycline | 128.52 | Ahmed et al. (2017) |
| Cocoa shell AC | Diclofenac | 63.47 | Saucier et al. (2015) |

phenolic compounds and pharmaceutics toward other adsorbents described in Tables 5 and 6.

## Conclusion

In this study, avocado seed was successfully used as raw material for producing activated carbons by conventional pyrolysis. In order to determine the best condition to produce the activated carbons, a DOE was employed by varying the temperature (500–700 °C) and time of pyrolysis (30–60 min).

The two evaluated factors (temperature and time of pyrolysis) strongly influenced the $S_{BET}$ and pore volume values; both factors had a negative effect which means that increasing the values of factors leads to decreases in $S_{BET}$ and pore volume values. The produced activated carbon exhibited high specific surface areas in the range of 1122–1584 $m^2$ $g^{-1}$. Surface characterisation revealed that ASACs have hydrophilic surfaces and have predominantly acidic groups on their surfaces.

The prepared ASACs were employed in the adsorption of 25 emerging organic compounds such as 10 pharmaceuticals and 15 phenolic compounds which presented high uptake values for all emerging pollutants. It was observed that the activated carbon prepared at higher temperature of pyrolysis (700 °C), which generated less total functional groups and presented higher HI, was the activated carbon with higher sorption capacity for uptaking emerging organic contaminants.

Based on results of this work, it is possible to conclude that avocado seed can be employed as a raw material to produce high surface area and very efficient activated carbons in relation to treatment of polluted waters with emerging organic pollutants.

**Acknowledgments** We are grateful to Chemaxon for giving us an academic research licence for the Marvin Sketch software, version 17.24.0 (http://www.chemaxon.com) 2017 used for emerging organic contaminant physical–chemical properties.

**Funding information** The authors gratefully thank the National Council for Scientific and Technological Development (CNPq, Brazil) and the

Coordination of Improvement of Higher Education personnel (CAPES, Brazil) for financial support of this work.

## References


Ahmed MJ, Islam MA, Asif M, Hameed BH (2017) Human hair-derived high surface area porous carbon material for the adsorption isotherm and kinetics of tetracycline antibiotics. Bioresour Technol 243:778–784. https://doi.org/10.1016/j.biortech.2017.06.174

Ahmed MB, Zhou JL, Ngo HH, Guo W, Chen M (2016) Progress in the preparation and application of modified biochar for improved contaminant removal from water and wastewater. Bioresour Technol 214:836–851. https://doi.org/10.1016/j.biortech.2016.05.057

Ba-Abbad MM, Takriff MS, Kadhum AAH, Mohamad AB, Benamor A, Mohammad AW (2017) Solar photocatalytic degradation of 2-chlorophenol with ZnO nanoparticles: optimisation with D-optimal design and study of intermediate mechanisms. Environ Sci Pollut Res 24(3):2804–2819. https://doi.org/10.1007/s11356-016-8033-y

Barbosa-Jr F, Krug FJ, Lima EC (1999) On-line coupling of electrochemical preconcentration in tungsten coil electrothermal atomic absorption spectrometry for determination of lead in natural waters. Spectrochim Acta B 54(8):1155–1166. https://doi.org/10.1016/S0584-8547(99)00055-5

Barbosa-Jr F, Lima EC, Krug FJ (2000) Determination of arsenic in sediment and soil slurries by electrothermal atomic absorption spectrometry using W-Rh permanent modifier. Analyst 125(11):2079–2083. https://doi.org/10.1039/b005783p

Beltrame KK, Cazetta AL, de Souza PSC, Spessato L, Silva TL, Almeida VC (2018) Adsorption of caffeine on mesoporous activated carbon fibers prepared from pineapple plant leaves. Ecotoxicol Environ Saf 147(2018):64–71. https://doi.org/10.1016/j.ecoenv.2017.08.034

Besha AT, Gebreyohannes AY, Tufa RA, Bekele DN, Curcio E, Giorno L (2017) Removal of emerging micropollutants by activated sludge process and membrane bioreactors and the effects of micropollutants on membrane fouling: a review. J Environ Chem Eng 5(3):2395–2414. https://doi.org/10.1016/j.jece.2017.04.027

Bhatnagar A, Anastopoulos I (2017) Adsorptive removal of bisphenol A (BPA) from aqueous solution: a review. Chemosphere 168:885–902. https://doi.org/10.1016/j.chemosphere.2016.10.121

Botomé ML, Poletto P, Junges J, Perondi D, Dettmer A, Godinho M (2017) Preparation and characterization of a metal-rich activated carbon from CCA-treated wood for $CO_2$ capture. Chem Eng J 321:614–621. https://doi.org/10.1016/j.cej.2017.04.004

Boudrahema N, Delpeux-Ouldriane S, Khenniche L, Boudrahema F, Aissani-Benissada F, Gineys M (2017) Single and mixture adsorption of clofibric acid, tetracycline and paracetamol onto activated carbon developed from cotton cloth residue. Process Saf Environ Prot 111:544–559. https://doi.org/10.1016/j.psep.2017.08.025

Bruns RE, Scarmino IS, de Barros-Neto B (2006) Statistical design—Chemometrics, First edn. Elsevier, Amsterdam

Calvete T, Lima EC, Cardoso NF, Dias SLP, Ribeiro ES (2010) Removal of brilliant green dye from aqueous solutions using home made activated carbons. CLEAN – Soil, Air, Water 38(5-6):521–532. https://doi.org/10.1002/clen.201000027

Carmalin AS, Lima EC, Allaudeen N, Rajan S (2016) Application of graphene based materials for adsorption of pharmaceutical traces from water and wastewater—a review. Desalin Water Treat 57:27573–27586

dos Reis GS, Adebayo MA, Sampaio CH, Lima EC, Thue PS, de Brum IAS, Dias SLP, Pavan FA (2017) Removal of phenolic compounds from aqueous solutions using sludge-based activated carbons prepared by conventional heating and microwave-assisted pyrolysis. Water Air Soil Pollut 228(33):1–17

dos Reis GS, Mahbub MKB, Wilhelm M, Lima EC, Sampaio CH, Saucier C, Dias SLP (2016a) Activated carbon from sewage sludge for removal of sodium diclofenac and nimesulide from aqueous solutions. Korean J Chem Eng 33(11):3149–3161. https://doi.org/10.1007/s11814-016-0194-3

dos Reis GS, Sampaio CH, Lima EC, Wilhelm M (2016b) Preparation of novel adsorbents based on combinations of polysiloxanes and sewage sludge to remove pharmaceuticals from aqueous solutions. Colloids Surf A Physicochem Eng Asp 497:304–315. https://doi.org/10.1016/j.colsurfa.2016.03.021

dos Reis GS, Wilhelm M, Silva TCA, Rezwan K, Sampaio CH, Lima EC, Souza SMAGU (2016c) The use of design of experiments for the evaluation of the production of surface-rich activated carbon from sewage sludge via microwave and conventional pyrolysis. Appl Therm Eng 93:590–597. https://doi.org/10.1016/j.applthermaleng.2015.09.035

Ennaciri K, Bacaoui A, Sergent M, Yaacoubi A (2014) Application of fractional factorial and Doehlert designs for optimizing the preparation of activated carbons from Argan shells. Chemometr Intell Lab 139:48–57. https://doi.org/10.1016/j.chemolab.2014.09.006

Fatta-Kassinos D, Michael C (2013) Wastewater reuse applications and contaminants of emerging concern. Environ Sci Pollut Res 20(6):3493–3495. https://doi.org/10.1007/s11356-013-1699-5

Geissena V, Mol H, Klumpp E, Umlauf G, Nadal M, van der Ploeg M, van de Zee SEATM, Ritsema CJ (2015) Emerging pollutants in the environment: a challenge for water resource management. Inter Soil Water Conser Res 3(1):57–65. https://doi.org/10.1016/j.iswcr.2015.03.002

Ghattas AK, Fischer F, Wick A, Ternes TA (2017) Anaerobic biodegradation of (emerging) organic contaminants in the aquatic environment. Water Res 116:268–295. https://doi.org/10.1016/j.watres.2017.02.001

Gil A, Garcia AM, Fernandez M, Vicente MA, Gonzalez-Rodriguez B, Rives V, Korili AS (2017) Effect of dopants on the structure of titanium oxide used as a photocatalyst for the removal of emergent contaminants. J Ind Eng Chem 53:183–191. https://doi.org/10.1016/j.jiec.2017.04.024

Giraldo L, Moreno-Piraján JC (2014) Study of adsorption of phenol on activated carbons obtained from eggshells. J Anal Appl Pyrol 106:41–47. https://doi.org/10.1016/j.jaap.2013.12.007

Goertzen SL, Theriault KD, Oickle AM, Tarasuk AC, Andreas HA (2010) Standardization of the Boehm titration. Part I. $CO_2$ expulsion and endpoint determination. Carbon 48(4):1252–1261. https://doi.org/10.1016/j.carbon.2009.11.050

Guo R, Guo J, Yu F, Gang DD (2013) Synthesis and surface functional group modifications of ordered mesoporous carbons for resorcinol removal. Microporous Mesoporous Mater 175(2013):141–146. https://doi.org/10.1016/j.micromeso.2013.03.028

Gupta VK, Nayak A, Agarwal S, Tyagi I (2014) Potential of activated carbon from waste rubber tire for the adsorption of phenolics: effect of pre-treatment conditions. J Colloid Interface Sci 417:420–430. https://doi.org/10.1016/j.jcis.2013.11.067

Isichei TO, Okieimen FE (2014) Adsorption of 2-nitrophenol onto water hyacinth activated carbon-kinetics and equilibrium studies. Environ Pollution 3:99–111

Jiang J-Q, Zhou Z, Sharma VK (2013) Occurrence, transportation, monitoring and treatment of emerging micro-pollutants in waste water—a review from global. Microchem J 110:292–300. https://doi.org/10.1016/j.microc.2013.04.014

Kishimoto N, Kobayashi M (2016) Effects of three additives on the removal of perfluorooctane sulfonate (PFOS) by coagulation using ferric chloride or aluminum sulfate. Water Sci Technol 73(12):2971–2977. https://doi.org/10.2166/wst.2016.161

Larous S, Meniai A-H (2016) Adsorption of diclofenac from aqueous solution using activated carbon prepared from olive stones. Int J Hydrog Energy 41(24):10380–10390. https://doi.org/10.1016/j.ijhydene.2016.01.096

Leite AJB, Sophia AC, Thue PS, dos Reis GS, Dias SLP, Lima EC, Vaghetti JCP, Pavan FA, de Alencar WS (2017) Activated carbon from avocado seeds for the removal of phenolic compounds from aqueous solutions. Desalin Water Treat 71:168–181. https://doi.org/10.5004/dwt.2017.20540

Lemraski EG, Sharafinia S, Alimohammadi M (2017) New activated carbon from Persian mesquite grain as an excellent adsorbent. Phys Chem Res 5:81–98

Lima EC, Adebayo MA, Machado FM (2015) Chapter 4—experimental adsorption in carbon nanomaterials as adsorbents for environmental and biological applications, Bergmann CP, Machado FM editors, Springer pp.71-84. DOI https://doi.org/10.1007/978-3-319-18875-1_4

Lima EC, Barbosa-Jr F, Krug FJ (2000) The use of tungsten–rhodium permanent chemical modifier for cadmium determination in decomposed samples of biological materials and sediments by electrothermal atomic absorption spectrometry. Anal Chim Acta 409(1-2):267–274. https://doi.org/10.1016/S0003-2670(99)00861-2

Lima EC, Barbosa-Jr F, Krug FJ (2001) Lead determination in biological material slurries by ETAAS using W-Rh permanent modifier. Fres J Anal Chem 369(6):496–501. https://doi.org/10.1007/s002160000667

Lin L, Jiang W, Xu P (2017c) Comparative study on pharmaceuticals adsorption in reclaimed water desalination concentrate using biochar: impact of salts and organic matter. Sci Total Environ 601–602:857–864

Lin L, Wang H, Jiang W, Mkaouar RA, Xu P (2017a) Comparison study on photocatalytic oxidation of pharmaceuticals by $TiO_2$-Fe and $TiO_2$-reduced graphene oxide nanocomposites immobilized on optical fibers. J Hazard Mat 333:162–168. https://doi.org/10.1016/j.jhazmat.2017.02.044

Lin L, Wang H, Xu P (2017b) Immobilized TiO2-reduced graphene oxide nanocomposites on optical fibers as high performance photocatalysts for degradation of pharmaceuticals. Chem Eng J 310:389–398. https://doi.org/10.1016/j.cej.2016.04.024

Matamoros V, Salvado V (2013) Evaluation of a coagulation/flocculation-lamellar clarifier and filtration-UV-chlorination reactor for removing emerging contaminants at full-scale wastewater treatment plants in Spain. J Environ Manag 117:96–102. https://doi.org/10.1016/j.jenvman.2012.12.021

Montgomery DC (2017) Design and analysis of experiments, 9th edn. John Wiley & Sons, New York

Petrova B, Tsyntsarski B, Budinovaa T, Petrova N, Velasco LF, Ania CO (2011) Activated carbon from coal tar pitch and furfural for the removal of p-nitrophenol and m-aminophenol. Chem Eng J 172(1):102–108. https://doi.org/10.1016/j.cej.2011.05.075

Prenzel T, Döge K, Motta RPO, Wilhelm M, Rezwan K (2014) Controlled hierarchical porosity of hybrid ceramics by leaching water soluble templates and pyrolysis. J Eur Ceram Soc 34(6):1501–1509. https://doi.org/10.1016/j.jeurceramsoc.2013.11.033

Prola LDT, Acayanka E, Lima EC, Umpierres CS, Vaghetti JCP, Santos WO, Laminsi S, Njifon PT (2013a) Comparison of Jatropha curcas shells in natural form and treated by non-thermal plasma as biosorbents for removal of Reactive Red 120 textile dye from aqueous solution. Ind Crop Prod 46:328–340. https://doi.org/10.1016/j.indcrop.2013.02.018

Prola LDT, Machado FM, Bergmann CP, de Souza FE, Gally CR, Lima EC, Adebayo MA, Dias SLP, Calvete T (2013b) Adsorption of Direct Blue 53 dye from aqueous solutions by multi-walled carbon nanotubes and activated carbon. J Environ Manag 130:166–175. https://doi.org/10.1016/j.jenvman.2013.09.003

Pubchem 2017: https://pubchem.ncbi.nlm.nih.gov/ site visited on September 27th, 2017

Puchana-Rosero MJ, Lima EC, Ortiz-Monsalve S, Mella B, da Costa D, Poll E, Gutterres M (2017) Fungal biomass as biosorbent for the removal of Acid Blue 161 dye in aqueous solution. Environ Sci Pollut Res 24(4):4200–4209. https://doi.org/10.1007/s11356-016-8153-4

Puchana-Rosero MJ, Adebayo MA, Lima EC, Machado FM, Thue PS, Vaghetti JCP, Umpierres CS, Gutterres M (2016) Microwave-assisted activated carbon obtained from the sludge of tannery-treatment effluent plant for removal of leather dyes. Colloids Surf A: Physicochem Eng Aspects 504:105–115. https://doi.org/10.1016/j.colsurfa.2016.05.059

Ren H, Shou W, Ren C, Gang DD (2016) Preparation and post-treatments of ordered mesoporous carbons (OMC) for resorcinol removal. Int J Environ Sci Technol 13(6):1505–1514. https://doi.org/10.1007/s13762-016-0990-7

Ribas MC, Adebayo MA, Prola LDT, Lima EC, Cataluna R, Feris LA, Machado FM, Pavan FA, Calvete T (2014) Comparison of a home-made cocoa shell activated carbon with commercial activated carbon for the removal of reactive violet 5 dye from aqueous solutions. Chem Eng J 248:315–326. https://doi.org/10.1016/j.cej.2014.03.054

Rossner A, Snyder SA, Knappe DRU (2009) Removal of emerging contaminants of concern by alternative adsorbents. Water Res 43(15):3787–3796. https://doi.org/10.1016/j.watres.2009.06.009

Rovani S, Rodrigues AG, Medeiros LF, Cataluña R, Lima EC, Fernandes AN (2016) Synthesis and characterisation of activated carbon from agroindustrial waste—preliminary study of 17β-estradiol removal from aqueous solution. J Environ Chem Eng 4(2):2128–2137. https://doi.org/10.1016/j.jece.2016.03.030

Saucier C, Adebayo MA, Lima EC, Cataluna R, Thue PS, Prola LDT, Puchana-Rosero MJ, Machado FM, Pavan FA, Dotto GL (2015) Microwave-assisted activated carbon from cocoa shell as adsorbent for removal of sodium diclofenac and nimesulide from aqueous effluents. J Hazard Mater 289:18–27. https://doi.org/10.1016/j.jhazmat.2015.02.026

Saucier C, Karthickeyan P, Ranjithkumar V, Lima EC, dos Reis GS, de Brum IAS (2017) Efficient removal of amoxicillin and paracetamol from aqueous solutions using magnetic activated carbon. Environ Sci Pollut Res 24(6):5918–5932. https://doi.org/10.1007/s11356-016-8304-7

Shou W, Chao B, Ahmad ZU, Gang DD (2016) Ordered mesoporous carbon preparation by the in situ radical polymerization of acrylamide and its application for resorcinol removal. J Appl Polym Sci 133(19). https://doi.org/10.1002/APP.43426

Strachowski P, Bystrzejewski M (2016) Comparative studies of sorption of phenolic compounds onto carbon-encapsulated iron nanoparticles, carbon nanotubes and activated carbon. J Mol Liq 213:351–359

Suresh S, Srivastava VC, Mishra IM (2011) Study of catechol and resorcinol adsorption mechanism through granular activated carbon: characterization, pH and kinetic study. Sep Sci Technol 46(11):1750–1766. https://doi.org/10.1080/01496395.2011.570284

Takdastan A, Mahvi AH, Lima EC, Shirmardi M, Babaei AA, Goudarzi G, Neisi A, Farsani MH, Vosoughi M (2016) Preparation, characterization, and application of activated carbon from low-cost material for the adsorption of tetracycline antibiotic from aqueous solutions. Water Sci Technol 74(10):2349–2363. https://doi.org/10.2166/wst.2016.402

Thommes M, Kaneko K, Neimark AV, Olivier JP, Rodriguez-Reinoso F, Rouquerol J, Sing KSW (2015) Physisorption of gases, with special reference to the evaluation of surface area and pore size distribution (IUPAC Technical Report). Pure Appl Chem 87:1051–1069

Thue PS, Adebayo MA, Lima EC, Sieliechi JM, Machado FM, Dotto GL, Vaghetti JCP, Dias SLP (2016) Preparation, characterization and application of microwave-assisted activated carbons from wood chips for removal of phenol from aqueous solution. J Mol Liq 223:1067–1080. https://doi.org/10.1016/j.molliq.2016.09.032

Thue PS, dos Reis GS, Lima EC, Sieliechi JM, Dotto GL, Wamba AGN, Dias SLP, Pavan FA (2017) Activated carbon obtained from sapelli

wood sawdust by microwave heating for o-cresol adsorption. Res Chem Intermed 43(2):1063–1087. https://doi.org/10.1007/s11164-016-2683-8

Umpierres CS, Prola LDT, Adebayo MA, Lima EC, dos Reis GS, Kunzler DDF, Dotto GL, Arenas LT, Benvenutti EV (2017) Mesoporous $Nb_2O_5/SiO_2$ material obtained by sol–gel method and applied as adsorbent of crystal violet dye. Environ Technol 38(5): 566–578. https://doi.org/10.1080/09593330.2016.1202329

Wang M, Li G, Huang LH, Xue J, Liu Q, Bao N, Huang J (2017) Study of ciprofloxacin adsorption and regeneration of activated carbon prepared from Enteromorpha prolifera impregnated with H3PO4 and sodium benzenesulfonate. Ecotox Environ Safe 139:36–42. https://doi.org/10.1016/j.ecoenv.2017.01.006

Yang G, Chen H, Qin H, Feng Y (2014) Amination of activated carbon for enhancing phenol adsorption: effect of nitrogen-containing functional groups. Appl Surf Sci 293:299–305. https://doi.org/10.1016/j.apsusc.2013.12.155

Yang J, Jin YX, Yu XP, Yue QF (2017) High surface area ordered mesoporous carbons from waste polyester: effective adsorbent for organic pollutants from aqueous solution. J Sol-Gel Sc Technol 83(2):413–421. https://doi.org/10.1007/s10971-017-4419-7

Zhang BP, Han XL, Gu PJ, Fang SQ, Bai J (2017a) Response surface methodology approach for optimization of ciprofloxacin adsorption using activated carbon derived from the residue of desilicated rice husk. J Mol Liq 238:316–325. https://doi.org/10.1016/j.molliq.2017.04.022

Zhang YJ, Zhu H, Szewzyk U, Lubbecke S, Geissen SU (2017b) Removal of emerging organic contaminants with a pilot-scale biofilter packed with natural manganese oxides. Chem Eng J 317: 454–460. https://doi.org/10.1016/j.cej.2017.02.095

Zhuo N, Lan Y, Yang W, Yang Z, Li X, Zhou X, Liu Y, Shen J, Zhang X (2017) Adsorption of three selected pharmaceuticals and personal care products (PPCPs) onto MIL-101(Cr)/natural polymer composite beads. Sep Purif Technol 177:272–280. https://doi.org/10.1016/j.seppur.2016.12.041

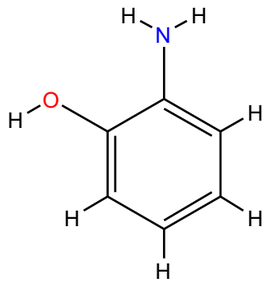

2-aminophenol

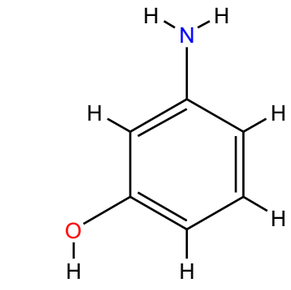

3-aminophenol

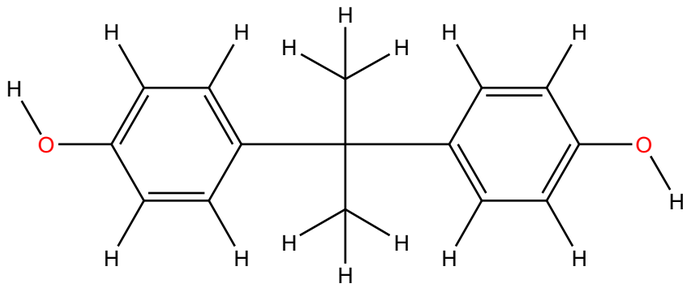

bisphenol A

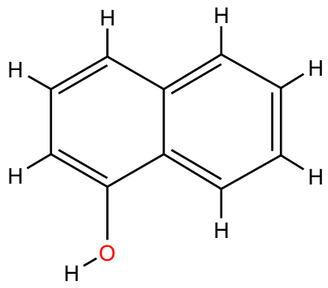

1-Naphtol

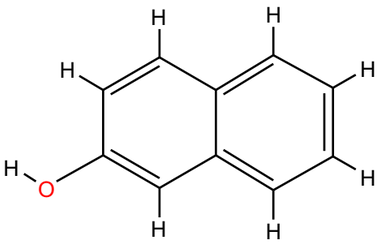

2-Naphtol

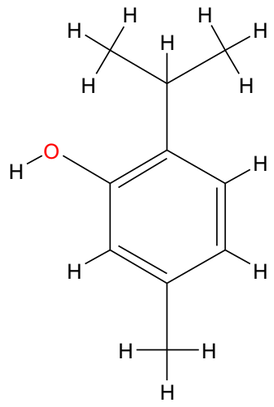

Thymol

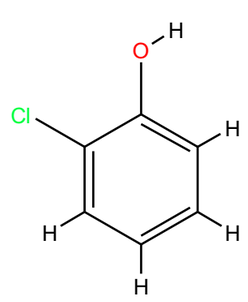

2-chlorophenol

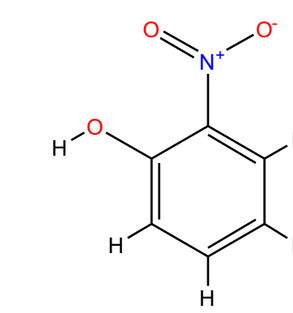

2-nitrophenol

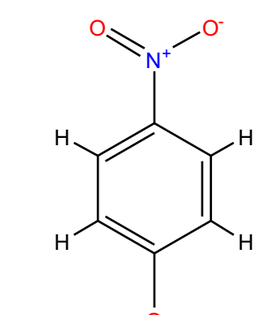

4-nitrophenol

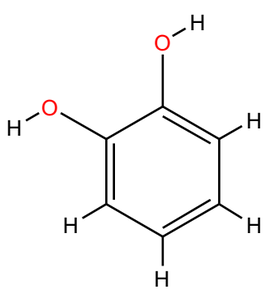

Cathecol

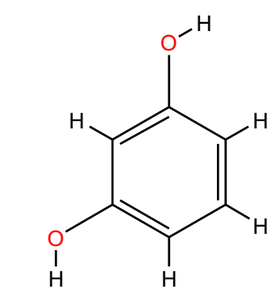

Resorcinol

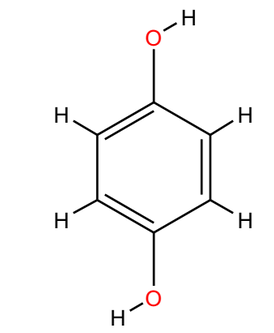

hydroquinone

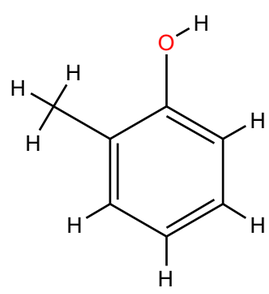

o-cresol

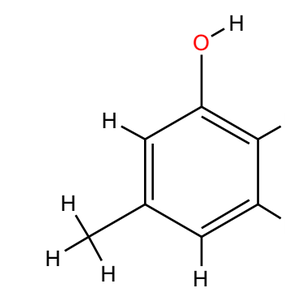

m-cresol

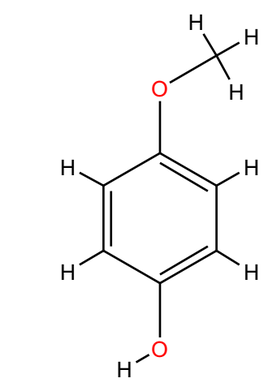

4-methoxyphenol

Supplementary Fig 1. Chemical structures of phenols.

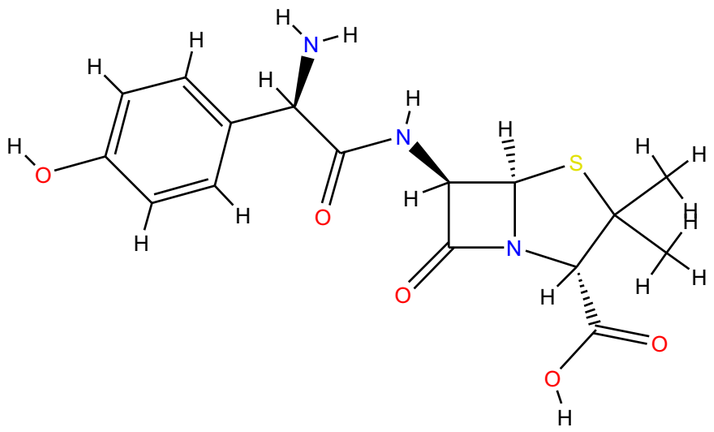

Amoxicilin

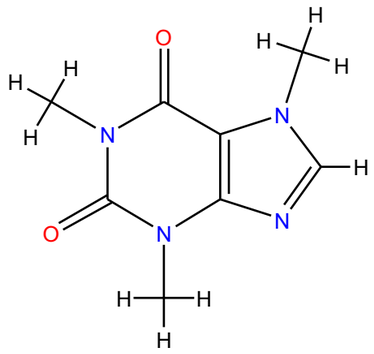

Caffein

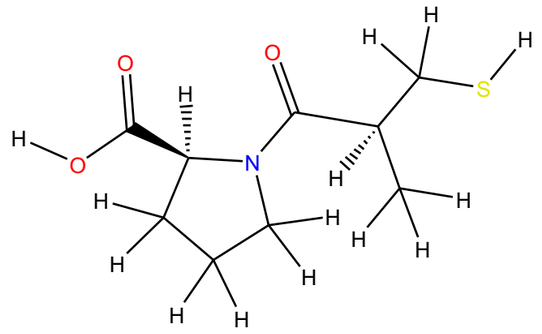

Captopril

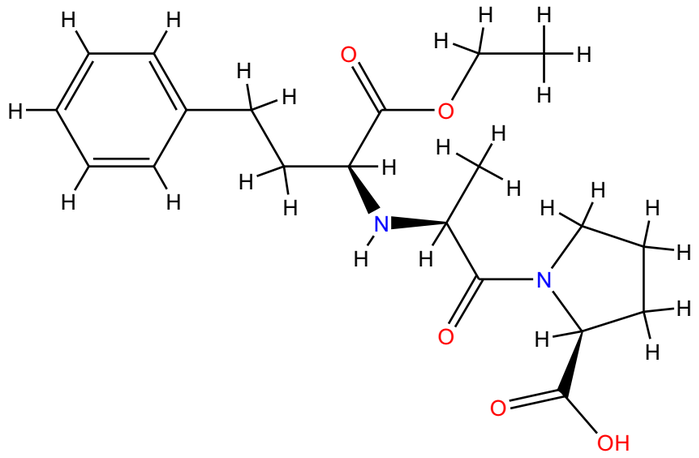

Enalapril

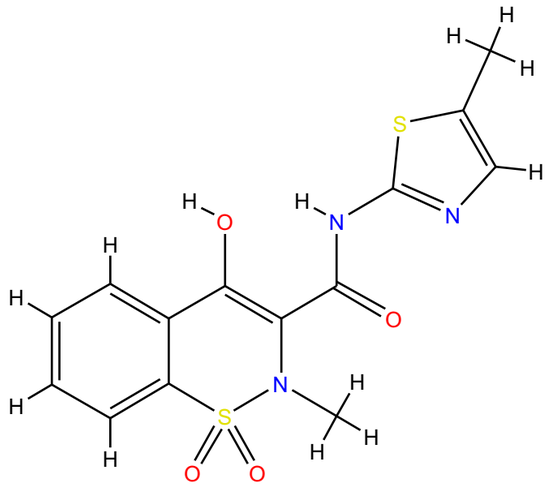

Meloxican

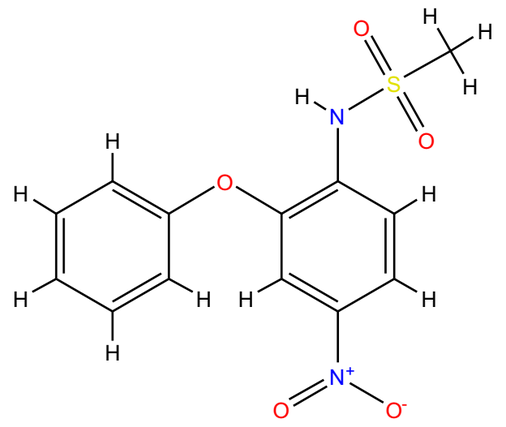

Nimesulide

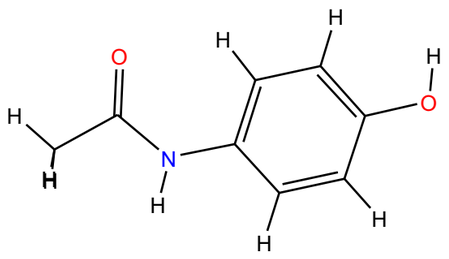

Paracetamol

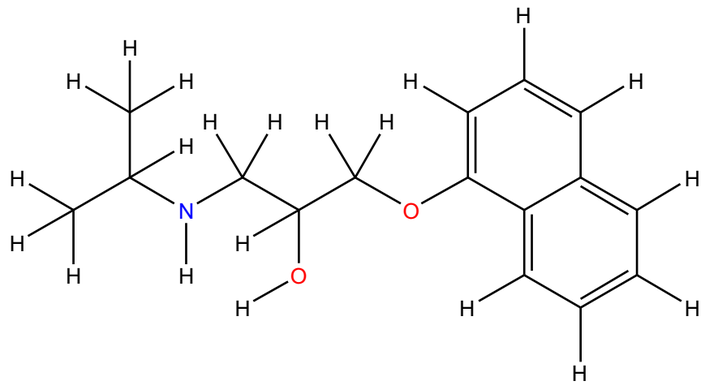

Propanolol

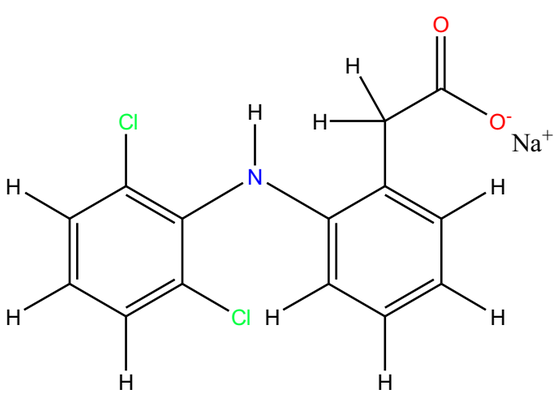

Sodium Diclofenac

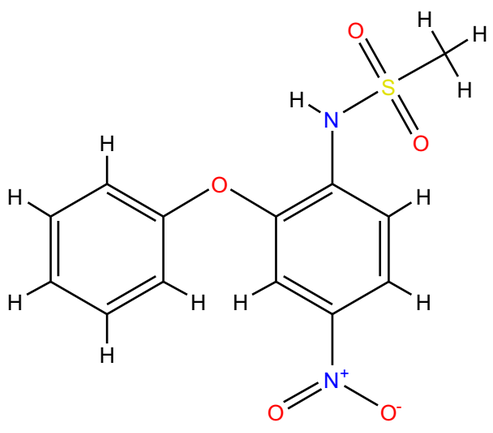

Tetracycline

Supplementary Fig 2. Chemical stuctures of pharmaceuticals

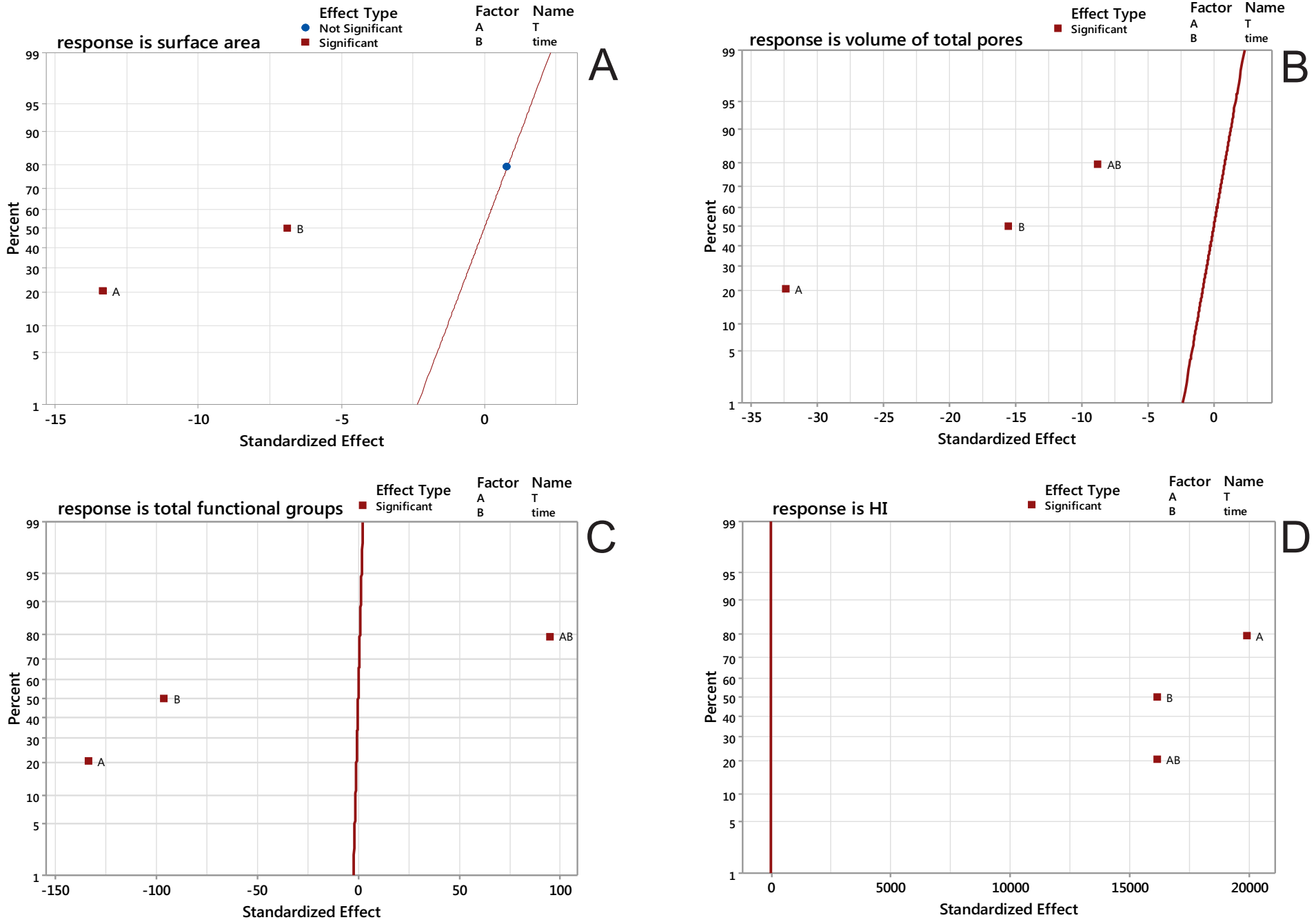


Supplementary Fig 3. Normal probability plot of standardized effects. Internal caption: A- final temperature of pyrolysis, B- holding time at final temperature of pyrolysis; A.B interaction of two factors. All red squares are significant, and all blue circle are not significant. The level of probability used in these graphs are 95%. A- response is surface area; B-response is total pore volume; C- total functional groups (acidic + basic); D- HI (hydrophobicity-hydrophilicity ratio).

Supplementary Table 1. Analysis of variance (ANOVA) for the coefficients temperature of pyrolysis (A) and time of holding at final temperature (B) on the responses for production of ASACs.

**Factorial Regression: $S_{BET}$ versus T; time; Center Point**

A

| Term | Coefficient | Standard Error of Coeff | Probability | Contribution (%) |
|---|---|---|---|---|
| Constant | $-7.66.10^{-4}$ | $6.10^{-6}$ | 0.000 | |
| T | $-8.6.10^{-5}$ | $6.10^{-6}$ | 0.006 | 77.90 |
| time | $-4.4.10^{-5}$ | $6.10^{-6}$ | 0.021 | 20.71 |
| Txtime | $5.10^{-6}$ | $6.10^{-6}$ | 0.512 | 0.27 |
| Center point | $7.10^{-6}$ | $1.0.10^{-5}$ | 0.534 | 0.24 |
| Error | | | | 0.88 |

$R^2$ 0.9912; $R^2_{adj}$ 0.9737

**Factorial Regression: Total volume of pores versus T; time; Center Point**

B

| Term | Coefficient | Standard Error of Coeff | Probability | Contribution (%) |
|---|---|---|---|---|
| Constant | -0.15618 | 0.00307 | 0.000 | |
| T | -0.09934 | 0.00307 | 0.001 | 71.28 |
| time | -0.04765 | 0.00307 | 0.004 | 16.40 |
| Txtime | -0.02692 | 0.00307 | 0.013 | 5.23 |
| Center point | 0.04741 | 0.00468 | 0.010 | 6.96 |
| Error | | | | 0.13 |

$R^2$ 0.9968; $R^2_{adj}$ 0.9959

**Factorial Regression: Total functional groups versus T; time; Center Poi.**

C

| Term | Coefficient | Standard Error of Coeff | Probability | Contribution (%) |
|---|---|---|---|---|
| Constant | -34874.9 | 0.00139 | 0.000 | |
| T | -0.18577 | 0.00139 | 0.000 | 41.42 |
| time | -0.13342 | 0.00139 | 0.000 | 21.37 |
| Txtime | 0.13169 | 0.00139 | 0.000 | 20.82 |
| Center point | -0.17849 | 0.00212 | 0.000 | 16.39 |
| Error | | | | 0.00 |

$R^2$ 1.000; $R^2_{adj}$ 0.9999

**Factorial Regression: HI versus T; time; Center Point**

D

| Term | Coefficient | Standard Error of Coeff | Probability | Contribution (%) |
|---|---|---|---|---|
| Constant | -302.417 | 0.000044 | 0.000 | |
| T | 0.881873 | 0.000044 | 0.000 | 36.47 |
| time | 0.715516 | 0.000044 | 0.000 | 24.01 |
| Txtime | 0.715489 | 0.000044 | 0.000 | 24.00 |
| Center point | -0.878954 | 0.000068 | 0.000 | 15.52 |
| Error | | | | 0.00 |

$R^2$ 1.000; $R^2_{adj}$ 1.000